

Interstellar polarization and extinction toward the Recurrent Nova T CrB[☆]

Yanko Nikolov*

Institute of Astronomy and National Astronomical Observatory, Bulgarian Academy of Sciences, Tsarigradsko Shose 72, Sofia, BG-1784, Bulgaria

Abstract

Spectropolarimetry is a powerful tool for diagnostic of interstellar matter and gives information on the geometry of the ejected material after the novae outbursts. In this paper are presented spectropolarimetric observations of the recurrent nova T CrB at quiescence obtained with FoReRo2 attached to the Cassegrain focus of the 2.0m RCC telescope of the Bulgarian Rozhen National Astronomical Observatory. The interstellar polarization toward T CrB was estimated using the field stars method. The spectropolarimetric observations were obtained from February 2018 to August 2021. In the wavelength range from 4800 Å to 8200 Å the maximum of the degree of linear polarization is $P_{max}(obs)(\%) = 0.46 \pm 0.01$ at $\lambda \approx 5200$ Å. The position angle is $PA_{.obs} = 100^\circ.8 \pm 0^\circ.9$. During the observations, there is no intrinsic polarization in T CrB, and the derived values represent interstellar polarization. The polarization toward T CrB is due to the foreground interstellar dust located at the distance up to ≈ 400 pc. Based on the degree of polarization the interstellar extinction toward the T CrB is $E_{B-V} \approx 0.07$.

Keywords: (ISM:) dust, extinction, Stars: binaries: symbiotic-individual: T CrB, techniques: polarimetric

1. Introduction

T CrB (HD 143454) is a symbiotic recurrent nova system. The Recurrent Novae (RNe) are a heterogeneous group of binary systems that have more than one recorded nova outburst. Two nova-like outbursts of T CrB in 1868 and 1946 are observed. There are currently 10 confirmed RNe in the Galaxy <Schaefer, 2010>. The presence of a massive, accreting white dwarf in the RNe systems makes them potential progenitors of Type Ia supernovae. T CrB consist of a massive white dwarf with $M_{WD} = 1.2-1.37 M_\odot$ (Belczynski & Mikolajewska <1998>, Stanishev et al. <2004>) and red giant with $M_{RG} \approx 1.12 M_\odot$ <Stanishev et al., 2004>. The orbital period of the binary is $227^d.57$ <Fekel et al., 2000>. Recurrent Novae are classified into long and short period systems <Anupama et al., 2013>. The donor of the long period systems is a red giant: RS Oph, T CrB, V3890 Sgr and V745 Sco. The short period systems are further divided into U Sco and T Pyx groups based on the outburst and quiescent properties <Anupama et al., 2013>. Reviews on the properties of RNe can be found

in Anupama <2008> and Schaefer <2010>.

Similar to RS Oph, T CrB is a symbiotic recurrent nova system. An intrinsic degree of polarization was observed two days after the last outburst of the recurrent nova RS Oph <Nikolov & Luna, 2021>. The intrinsic polarization is $\approx 1\%$ with well visible strong depolarization effects in H_α and He I 5876 emission lines. The position angle is aligned with the highly collimated outflows detected during the past outburst in 2006 <Rupen et al., 2008>. To obtain an intrinsic degree of polarization and position angle of the recurrent nova T CrB shorter after the upcoming outburst <Luna et al., 2020>, it is necessary to obtain the interstellar polarization toward T CrB.

In this study are presented spectropolarimetric observations of T CrB, obtained with the 2-Channel-Focal-Reducer Rozhen (FoReRo2) attached to the 2.0m RCC telescope of the Bulgarian Rozhen National Astronomical Observatory.

2. Observations and Data Analysis

Spectropolarimetric observations of T CrB were secured with the 2-Channel-Focal-Reducer Rozhen (FoReRo2) similar to that described by Jockers et al. <2000>, attached to the Cassegrain focus of the 2.0m

[☆]Based on data collected with 2-m RCC telescope at Rozhen National Astronomical Observatory.

*Corresponding author.

Email address: ynikolov@nao-rozhen.org (Yanko Nikolov)

RCC telescope of the Bulgarian Rozhen National Astronomical Observatory. A Super-Achromatic (in the range 3800 Å– 7900 Å) True Zero-Order Waveplate 5 retarder (APSAW-5)¹ has been added to FoReRo2. Polarized spectra are obtained at 8 retarder angles: 0°, 22.5°, 45°, 67.5°, 90°, 112.5°, 135° and 157.5°. A beam swapping technique is used (Bagnulo et al. <2009>, Nikolov et al. <2019>) to minimize instrumental polarization. Instrumental polarization is corrected using a standard star with zero degree of polarization. The offset between position angle in the celestial and instrumental polarization is corrected using strongly polarized standard stars. The observations were made from 2018 February 17 to 2021 August 08, covering the orbital period of T CrB. Polarized spectra of T CrB, the stars from the field of T CrB, and standard stars with high (HD 204827 and HD 161056, Schmidt et al. <1992>) and zero degrees of polarization (HD 212311 and HD 154892, Turnshak et al. <1990>) were obtained. Polarization standards and the stars from the field of T CrB were observed with the same instrumental setup as T CrB on the same nights. The spectra were reduced using IRAF <Tody, 1993> in the standard way including bias removal and wavelength calibration. The journal of observations is given in Table 1. The table contains: objects, the date (in format YYYYMMDD), UT of the middle of the observation, the total exposure time for all retarder angles, observed high and zero polarization standards, angular distance from T CrB and distance. The last column represents observed degree of polarization and position angle in synthetic V filter.

3. Results

3.1. Observed degree of polarization and position angle of T CrB

The observed degree of polarization and position angle in the wavelength range from 4800 Å to 8200 Å are plotted on Fig.1. The maximum of the degree of polarization is $P_{max}(obs)(\%) = 0.46 \pm 0.01$ at $\lambda \approx 5200$ Å. The angle of polarization has a flat behavior with no visible wavelength dependence and it has a value of $P.A._{obs} = 100^\circ.8 \pm 0^\circ.9$, where $P.A._{obs}$ represents an average value of all observed position angles of T CrB in synthetic V filter. The degree of polarization can be fit with Serkowski's law with coefficient $P_{max}=0.46$, $K=1.36$ and $\lambda_{max}=5194\text{Å}$.

The observed value of the Stokes parameters $Q_V(\%)$ and $U_V(\%)$ in synthetic V filter obtained in different orbital phases are presented in Fig.2. The orbital phase

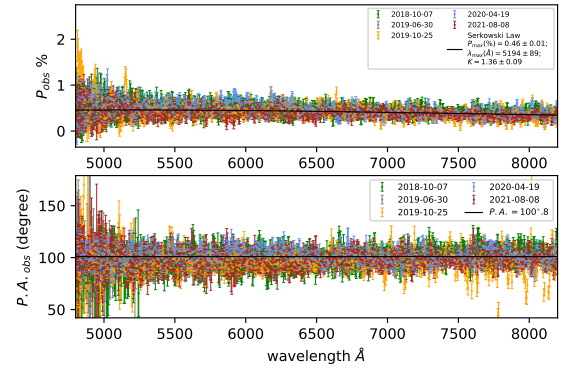


Figure 1: Degree of polarization and Position Angle of T CrB. Black curve represents fit with Serkowski's law with coefficients $P_{max}=0.46$, $K=1.36$ and $\lambda_{max}=5194\text{Å}$.

is calculated using $P_{orb} = 227.5678 \pm 0.0099$ days and $T_o = 2447918.62 \pm 0.27$, where T_o is the time of maximum velocity <Fekel et al., 2000>. Solid blue lines represent the average values of the Stokes parameters Q_V and U_V respectively. The semi-transparent bands represent errors of the Stokes parameters. During the observations between 2018 February 17 and 2021 August 08 the variable degree of polarization is not observed.

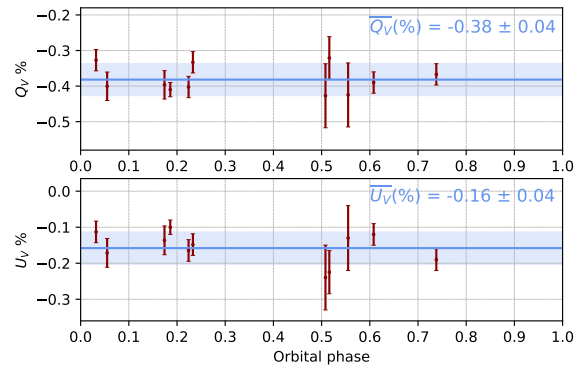


Figure 2: Orbital phase vs. Stokes Q_{obs} and Stokes U_{obs} in T CrB. The circles represent the observed data in the synthetic V band. The blue line represents the average value of Stokes Q_V and Stokes U_V parameter respectively. The semi-transparent bands determine areas with $\pm 1\sigma$ around the average values.

¹<http://astropribor.com/waveplates/>

Table 1: Journal of observations of T CrB and the stars from the field of T CrB.

Object	Date	UT	Exp. ^a (s)	Standards	Angular distance	Distance ^b pc	P _V (%)	P.A. _V [deg.]
T CrB	2018-02-17	01:24	960	1			0.35 ± 0.03 ^c	99.5 ± 2.0 ^c
	2018-10-07	17:41	720	2			0.44 ± 0.04 ^c	101.6 ± 2.6 ^c
	2019-06-30	22:11	1920	1			0.43 ± 0.02 ^c	101.1 ± 1.8 ^c
	2019-07-02	21:09	1440	1			0.36 ± 0.02 ^c	102.0 ± 2.0 ^c
	2019-10-25	17:21	960	2			0.41 ± 0.02 ^c	103.7 ± 1.8 ^c
	2020-02-02	01:27	240	1	–	887 ⁺¹⁸ ₋₂₉	0.42 ± 0.04 ^c	99.5 ± 2.9 ^c
	2020-04-18	02:11	144	1			0.49 ± 0.10 ^c	104.6 ± 5.4 ^c
	2020-04-19	20:22	240	1			0.48 ± 0.03 ^c	105.2 ± 1.8 ^c
	2020-04-28	19:46	192	1			0.41 ± 0.07 ^c	95.3 ± 5.8 ^c
	2021-05-04	20:41	1440	1			0.42 ± 0.02 ^c	97.2 ± 1.4 ^c
	2021-08-08	19:58	960	1			0.41 ± 0.03 ^c	98.9 ± 2.4 ^c
HD 143256	2020-02-02	01:38	480	1			0.41 ± 0.03 ^c	104.0 ± 2.2 ^c
	2020-04-19	20:31	960	1	14'	613 ⁺⁵ ₋₄	0.40 ± 0.03 ^c	106.5 ± 1.9 ^c
	2020-04-28	20:12	480	1			0.38 ± 0.03 ^c	96.1 ± 2.8 ^c
BD +26 2759	2020-02-02	01:53	240	1			0.33 ± 0.07 ^c	104.0 ± 4.7 ^c
	2020-04-19	20:54	320	1	22.3'	1066 ⁺²⁶ ₋₂₆	0.48 ± 0.06 ^c	107.4 ± 3.3 ^c
	2020-04-28	19:57	360	1			0.43 ± 0.06 ^c	95.5 ± 3.5 ^c
HD 143161	2020-02-02	02:10	480	1	23.6'	759 ⁺⁹ ₋₉	0.40 ± 0.02 ^c	103.1 ± 1.8 ^c
	2020-04-19	21:08	400	1			0.38 ± 0.04 ^c	107.3 ± 2.4 ^c
2MASS 16005644 +2550020	2020-02-02	02:32	1200	1			0.36 ± 0.06 ^c	101.5 ± 5.9 ^c
	2020-04-19	21:36	1200	1	20'	727 ⁺⁸ ₋₇	0.40 ± 0.07 ^c	75.5 ± 6.4 ^c
2MASS 16000301 +2555003	2020-02-02	02:58	1200	1	7.4'	919 ⁺¹³ ₋₁₁	0.32 ± 0.10 ^c	95.9 ± 26.0 ^c
HD 142762	2021-08-08	20:26	960	1	0.94°	278 ⁺² ₋₂	0.38 ± 0.01 ^c	99.4 ± 1.3 ^c
HD 142053	2021-08-08	20:57	480	1	1.91°	217 ⁺¹ ₋₁	0.47 ± 0.01 ^c	110.6 ± 1.0 ^c
HD 138749	2021-08-08	21:19	72	1	7.96°	121 ⁺² ₋₃	0.30 ± 0.01 ^c	93.7 ± 0.8 ^c

Note: ^a - Total exposure time; (1) - high polarization standard HD 161056 & zero polarization standard HD 154892; (2) - high polarization standard HD 204827 & zero polarization standard - HD 212311; ^b Distance based on Gaia DR3 <Bailer-Jones et al., 2021>.

3.2. Interstellar polarization toward the Recurrent Nova T CrB

The observed polarization is a vectorial sum of intrinsic polarization and interstellar polarization. When the intrinsic polarization of the observed objects is zero, the observed polarization represents interstellar polarization. In the optical region, the degree of interstellar polarization is a function of the wavelength <Serkowski et al., 1975>:

$$P_{ISP}(\lambda) = P_{max} \exp\left(-K \ln^2 \frac{\lambda_{max}}{\lambda}\right), \quad (1)$$

where P_{max} is the peak of the interstellar polarization at wavelength λ_{max} .

In Table 2 is presented the parameters of the Serkowski's law for T CrB, HD 143256, BD +26 2759; HD 143161; HD 142762; HD 142053 and HD 138749. In this table are included only data with good S/N. The last two columns represent R_V and grain size a .

Interstellar polarization toward T CrB was estimated using the polarization of stars in the direction of T CrB. In Table 1 are given objects, angular distance from T CrB, distance <Bailer-Jones et al., 2021>, and the last two columns represent observed degree of polarization and position angle in synthetic V filter.

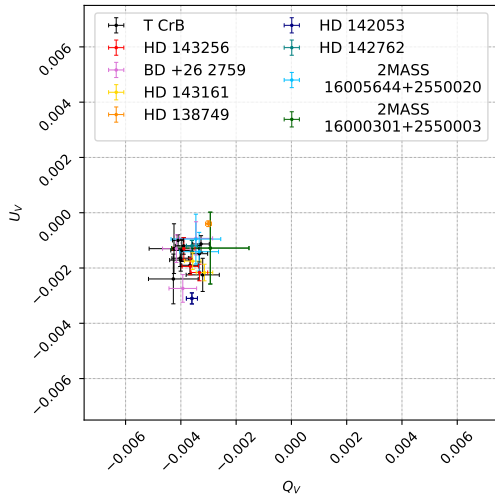


Figure 3: QU diagram of T CrB and stars from the field of T CrB.

In Fig.3 is presented a QU diagram of T CrB and stars from the field of T CrB. Observed Stokes parameters in synthetic V filter Q_V and U_V of T CrB have the same values as Stokes parameters Q_V and U_V of stars from the field of T CrB. In Fig.4 are presented the observed degree of polarization and position angle of T CrB and

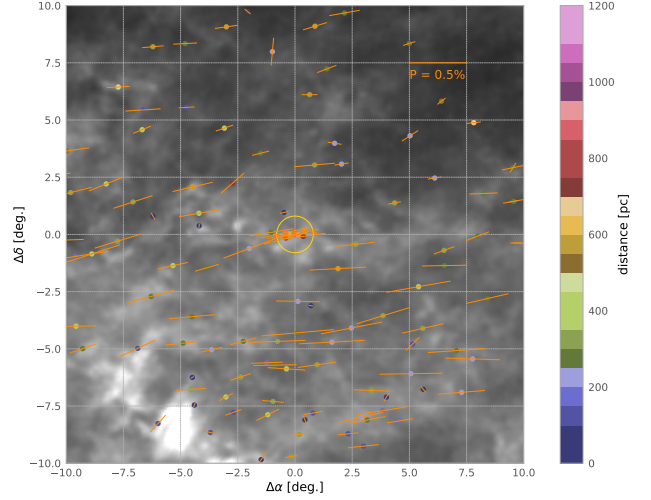


Figure 4: The interstellar polarization of the field stars around T CrB (Heiles <2000>; Berdyugin et al. <2014>). The degree of polarization is proportional to the length of its bar. The horizontal bar of the top right presents 0.5% polarization. The P.A. of the stars of the direction of T CrB (inside of the yellow circle, Table 1) are similar to that of T CrB. The color of every star corresponds to its distance. The background image represents 100 μm dust emission maps <Schlegel et al., 1998>.

stars from the field of T CrB obtained on 2020 February 2. Fig.3 and Fig.4 indicate that observed polarization of T CrB represents interstellar polarization.

The relationship between the grain size and the wavelength of maximum polarization for long dielectric cylinders with radius a and refractive index n has been quantified by Whittet <2003> as:

$$\lambda_{max} \approx 2\pi a(n - 1), \quad (2)$$

where λ_{max} and a are expressed in μm . For silicate grains ($n=1.6$), $\lambda_{max} = 5194\text{\AA}$ yields a grain size of the order of $0.14 \mu\text{m}$ (last column of Table 3).

The linear relationship between total-to-selective extinction ratio R_V and the wavelength of maximum polarization was suggested by Whittet & van Breda <1978> as:

$$R_V = (5.6 \pm 0.3)\lambda_{max}, \quad (3)$$

where λ_{max} is expressed in μm . It is worth noting that this relationship is still debated (see Bagnulo et al. <2017>). Calculated values for R_V are presented in Table 2.

Table 2: The parameters of the Serkowski's law, R_V and grain size a .

Object	$P(\lambda)_{max}(\%)$	K	$\lambda_{max}(\text{\AA})$	R_V^a	$a(\mu\text{m})^b$
T CrB	0.46 ± 0.01	1.36 ± 0.09	$5194\text{\AA} \pm 89\text{\AA}$	2.9 ± 0.2	0.14
HD 143256	0.41 ± 0.01	1.15 ± 0.11	$6121\text{\AA} \pm 48\text{\AA}$	3.4 ± 0.5	0.16
BD +26 2759	0.39 ± 0.01	1.28 ± 0.22	$6012\text{\AA} \pm 125\text{\AA}$	3.4 ± 0.9	0.16
HD 143161	0.44 ± 0.01	1.12 ± 0.05	$5686\text{\AA} \pm 44\text{\AA}$	3.2 ± 0.4	0.15
HD 142762	0.36 ± 0.01	2.01 ± 0.02	$5419\text{\AA} \pm 12\text{\AA}$	3.0 ± 0.2	0.14
HD 142053	0.49 ± 0.01	1.4 ± 0.02	$5324\text{\AA} \pm 13\text{\AA}$	3.0 ± 0.2	0.14
HD 138749	0.26 ± 0.01	0.76 ± 0.02	$5497\text{\AA} \pm 20\text{\AA}$	3.1 ± 0.3	0.15

Note: ^a - R_V calculated with eq.3; ^b - grain size calculated with eq. 2.

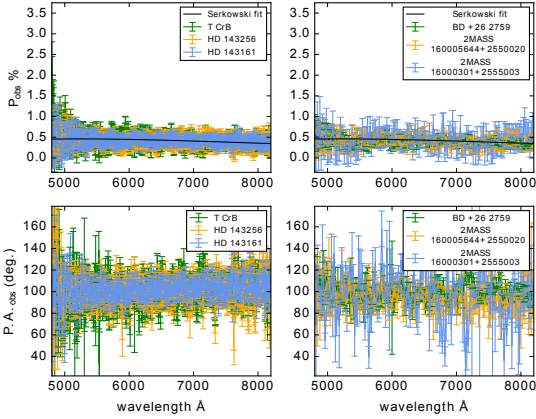


Figure 5: Observed degree of polarization and position angle of T CrB and stars of the direction of T CrB on 2020 February 2. Black curve represents fit with Serkowski law with coefficients $P_{max}=0.46$, $K=1.36$ and $\lambda_{max}=5194\text{\AA}$.

3.3. Polarization vs. distance

The behavior of $P(\%)$ with distance (in Kpc) is described with the equation <Fosalba et al., 2002>:

$$P(\%) \approx 0.13 + 1.81d - 0.47d^2 + 0.036d^3, \quad (4)$$

where d is in Kpc.

In Fig.6 the grey and black dots represent stars at an angular distance less than 10 degrees from T CrB. The data are taken from Heiles <2000> and Berdyugin et al. <2014>. Both catalogs: "Stellar polarization catalogs agglomeration" <Heiles, 2000> and "Polarization at high galactic latitude" <Berdyugin et al., 2014> include relatively bright stars at the distance up to 600 pc in the field 10×10 deg. around T CrB. In Fig.6 the distance to those stars is based on Gaia DR3 <Bailer-Jones et al., 2021>. The orange line represents the polarization vs. distance relationship <Fosalba et al., 2002> and

is described with eq. 4. The behavior of $P(\%)$ with the distance well describes the observed data at the distance up to 300 pc as well visible in Fig.6. The scatter of the data depends on the local characteristics of the interstellar medium. This is well visible in Fig.4, where the background image represents $100 \mu\text{m}$ dust emission map <Schlegel et al., 1998>.

The degree of polarization in the direction toward T CrB is practically constant at the distance from 400 pc to 1100 pc. The angular distance of HD 143256; BD +26 2759; HD 143161; 2MASS 16005644 +2550020 and 2MASS 16000301 +2555003 from T CrB is in range from $7'$ to $24'$ (inside the yellow circle in Fig.4), accordingly those stars are practically in the direction of T CrB. This behavior of the degree of polarization between 400 and 1100 pc can be explained with a low-density cavity of the interstellar dust around T CrB. It can be concluded that the polarization toward T CrB is due to the foreground interstellar dust located at the distance up to ≈ 400 pc.

3.4. Comparison with catalogs

For the three stars: HD 138749 <Heiles, 2000>, HD 142053, and HD142762 <Berdyugin et al., 2014> were obtained spectropolarimetric observations on 2021 August 08. The synthetic V filter was used for comparison with both catalogs. The results are demonstrated in table 3. HD 138749 is classified as Be stars. Be stars are characterized with an intrinsic degree of polarization <Clarke, 2010>. In the observations obtained on 2021-08-08, the H_α line is in absorption - there is no circumstellar disc around Be stars, for this reason, most probably the observed polarization represents interstellar polarization. In Heiles's catalog the degree of polarization of HD 138749 is $0 \pm 0.2\%$ and if the star has intrinsic polarization in this moment of observations the intrinsic component of polarization would be $P_{int} \approx 0.30\%$ at position angle $\approx 4^\circ$.

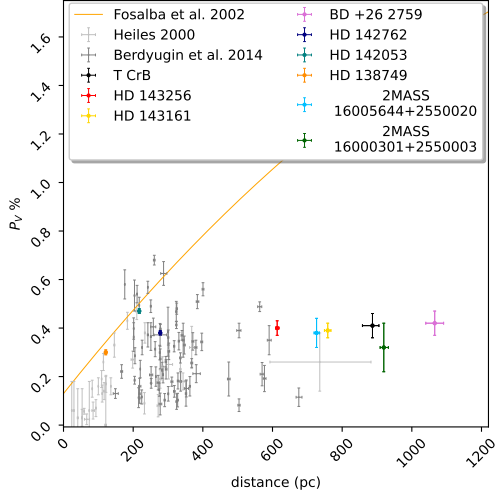


Figure 6: Polarization vs. distance. The orange line represents the polarization vs. distance relationship <Fosalba et al., 2002>.

HD 142053 and HD142762 <Berdyugin et al., 2014> were chosen because their P.A. is different from the general trend of the P.A. of the stars of the field of T CrB. The values of P.A. presented in this paper are very close to the general trend - in Fig.4 both stars are closest to the yellow circle. In Fig.7 is presented observed degree of polarization and position angle for these three stars: HD 138749; HD 142053 and HD142762. The dark orange lines represent fit with Serkowski's law. It is interesting to mention that the K coefficient of the Serkowski law is slightly different from 1.15 (the K coefficient of the original work of Serkowski et al. <1975> for two of these stars: HD 142762 and HD138749 (see Table 3).

3.5. Interstellar extinction

Two main components of the interstellar medium are gas and interstellar dust grains.

3.5.1. Estimates of E_{B-V} from diffuse interstellar bands (DIBs)

The Diffuse Interstellar Bands (DIBs) represent hundreds of weak absorption features in the wavelength range between ~ 4000 and $10\,000$ Å. DIBs are first mentioned in the work of Heger <Heger, 1919>. Until now over 400 DiBs are registered <Hobbs et al., 2009>. The correlation between equivalent width (EW) of the DIBs and E_{B-V} was suggested by Puspitarini et al. <2013>. The EW of two DIBs centered at 5780Å and 5797Å were used to determine E_{B-V} . In the 10×10 deg. field around T CrB has used eleven stars of the "Probing the Local Bubble with DIBs" catalog <Farhang et al.,

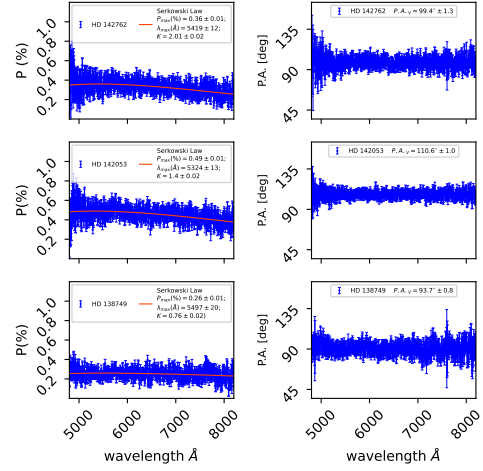


Figure 7: Observed degree of polarization and position angle of three stars of the Heiles's and Berdyugin's catalog. The dark orange lines represent fit with Serkowski's law.

2015>. The following equations were used to determine interstellar extinction toward those stars <Puspitarini et al., 2013>:

$$E_{B-V} = (0.0086 \pm 0.0054) + (0.0023 \pm 0.0001)EW_{5780} \quad (5)$$

$$E_{B-V} = (0.0203 \pm 0.0172) + (0.0063 \pm 0.0005)EW_{5797} \quad (6)$$

where EW is in mÅ.

The values of the E_{B-V} are presented in Table 4. The Table 4 contains: objects, EW_{5780} and EW_{5797} and corresponding E_{B-V} obtained with equations 5 and 6. The last two columns represent the degree of polarization and E_{B-V} calculated with equation 8.

3.5.2. Estimates E_{B-V} from degree of polarization

The relationships between polarization and distance and polarization and extinction have been quantified by Fosalba et al. <2002> with the following equations:

$$P(\%) \approx 0.13 + 1.81d - 0.47d^2 + 0.036d^3, \quad (7)$$

where d is distance in Kpc.

$$P(\%) \approx 3.5E(B-V)^{0.8}. \quad (8)$$

The distance to T CrB is 0.887 Kpc <Bailer-Jones et al., 2021> so that using equation 7 is obtained $P(\%) \approx 0.79$. Toward T CrB $E_{B-V} = 0.15$ <Cassatella et al.,

Table 3: Comparison with catalogs

Object	Angular distance from T CrB [deg.]	Spectral class	$Distance^a$ [pc]	Catalogue		This work	
				P_V (%)	P.A. [deg.]	P_V (%)	P.A. [deg.]
HD 142762	0.94	K0	278^{+2}_{-2}	0.273 ± 0.041^b	169.0 ± 4.0^b	0.38 ± 0.01	99.4 ± 1.3
HD 142053	1.91	KIII	217^{+1}_{-1}	0.494 ± 0.033^b	165.0 ± 2.0^b	0.47 ± 0.01	110.6 ± 1.0
HD 138749	7.96	B6Vnne	121^{+2}_{-3}	0.0 ± 0.2^c	0.0 ± 90.0^c	0.30 ± 0.01	93.7 ± 0.8

Note: ^a Distance based on Gaia DR3 <Bailer-Jones et al., 2021>; ^b Polarization at high galactic latitude <Berdyugin et al., 2014>; ^c Stellar polarization catalogs agglomeration <Heiles, 2000>. The spectral class are taken from SIMBAD database.

1982> so that $P(\%) \approx 0.77$ Observed maximum of a degree of polarization of T CrB $P(\lambda)_{max}(\%) = 0.46 \pm 0.01$ is lower that calculated using eq. 7 and eq. 8. This is another argument in favor of low-density cavity of the interstellar dust around T CrB.

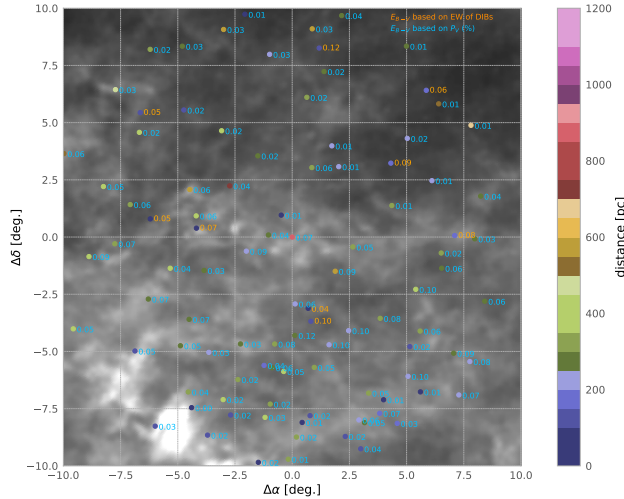


Figure 8: The interstellar extinction of the stars in the field around T CrB. The color of every star corresponds to its distance. The background image represents $100 \mu\text{m}$ dust emission maps <Schlegel et al., 1998>.

The interstellar extinction of the field stars around T CrB is presented in Fig.8. With blue color are presented E_{B-V} obtained with equation 8. The degree of polarization is taken from: "Stellar polarization catalogs agglomeration" <Heiles, 2000>, "Polarization at high galactic latitude" <Berdyugin et al., 2014> and this work (Table 1). With orange color are presented E_{B-V} based on EW of DIBs 5780\AA and 5797\AA . The color of every star corresponds to its distance.

For four of the stars presented in Table 4 we can compare the E_{B-V} obtained with EW of DIBs (eq. 5 and

eq.6) and degree of polarization (eq. 8). Only the star - HD 138749 has a close values of E_{B-V} obtained by two methodics. A previous study based on spectropolarimetric observations of DIBs in the spectral range from 4480\AA to 6620\AA , Cox et al. <2007> concluded that DIBs do not originate from grains, but they are rather large gas phase molecules that can survive in the diffuse interstellar medium. So the results presented in Table 4 are not unusual and can be explained by the various causes of extinction due to the DIBs and dust.

3.6. Spectral classification of the stars in the direction of T CrB

Optical spectra (Stokes I) of T CrB and the stars of the direction of T CrB, obtained in 2020 February 2 are shown in Fig.9. Spectrophotometric standard star 108 Vir was used for flux calibration. All fluxes were corrected for interstellar reddening of $E_{B-V} = 0.07$ using the extinction law by Cardelli et al. <1989>. Spectral classification of observed stars has been performed with the python package PyHammer <Kesseli et al., 2017>. PyHammer determines the spectral type of the object by comparing various spectral templates to the observed spectra. The spectral type of HD 143256 is K0 and the spectral type of HD 143161 is K2 <Cannon & Pickering, 1993>. For HD 143256 the best fit of spectra with PyHammer was obtained with spectral type K3. For HD 143161 the best fit of spectra with PyHammer was obtained with spectral type K7. The spectral type of T CrB is M4 III and $M_{bol}(mag) = -2.29$ <Schaefer, 2009>. Anupama & Mikołajewska <1999> obtained a spectral type of M3-4 III for the M giant in T CrB. For T CrB the best fit of spectra obtained 2020 February 2 corresponding to spectral type M3. Using bolometric correction for this spectral type <Pecaut & Mamajek, 2013> was calculated $M_{bol}(mag) = -2.02$.

Evaluation of V-band (m_v) and M_{bol} are presented in Table 5. Table 5 contain: magnitude in V band

Table 4: Interstellar extinction toward T CrB based on EW of DIBs and degree of polarization

Object	EW_{5780}^a [mÅ]	E_{B-V}^b [mag.]	EW_{5797}^a [mÅ]	E_{B-V}^c [mag.]	P_V (%)	E_{B-V}^f [mag.]
HD 143894	7.07 ± 1.71	0.02 ± 0.01	4.89 ± 1.36	0.05 ± 0.03		
HD 143992	41.53 ± 7.42	0.10 ± 0.03	12.42 ± 3.48	0.10 ± 0.05		
HD 140436	38.48 ± 5.82	0.10 ± 0.02	2.85 ± 1.2	0.04 ± 0.03	0.03 ± 0.12^d	0.003 ± 0.05
HD 146738	40.88 ± 6.13	0.10 ± 0.02	9.61 ± 2.45	0.08 ± 0.04		
HD 139006	–	–	4.09 ± 1.21	0.05 ± 0.03	0.06 ± 0.12	0.006 ± 0.05
HD 148554	33.04 ± 5.2	0.08 ± 0.02	7.77 ± 2.33	0.07 ± 0.04		
HD 140159	–	–	–	–	0.024 ± 0.022^d	0.002 ± 0.01
HD 138749	25.74 ± 4.37	0.07 ± 0.02	3.03 ± 0.97	0.04 ± 0.02	0.30 ± 0.01^e	0.046 ± 0.02
HD 147835	22.19 ± 4	0.06 ± 0.02	–	–		
HD 144359	35.37 ± 5.58	0.09 ± 0.02	19.57 ± 3.8	0.14 ± 0.05		
HD 150361	–	–	10.35 ± 2.22	0.09 ± 0.04		

Note: ^a "Probing the Local Bubble with DIBs" <Farhang et al., 2015>; ^b Interstellar extinction calculated with eq. 5; ^c Interstellar extinction calculated with eq. 6; ^d "Stellar polarization catalogs agglomeration" <Heiles, 2000>; ^e This work (Table 1); ^f Interstellar extinction calculated with eq. 8;

(m_v), distance based on Gaia DR3 <Bailer-Jones et al., 2021>, the absolute magnitude in V-band (M_V), Spectral type, Bolometric correction from Pecaut & Mamajek <2013> and the last column represents absolute bolometric magnitude (M_{bol}). V-band magnitudes (m_v) for T CrB from the American Association of Variable Star Observers (AAVSO) database for 2020-02-02 UTC 04:43:27 and 2020-02-03 UTC 04:05:03 are 9.768 ± 0.029 and 9.962 ± 0.002 , respectively. With sband IRAF procedure and using spectrophotometric standard star 108 Vir was obtained for T CrB $m_v = 9.9$ on date 2020-02-02.

Discussion

The polarized light coming from astronomical objects brings important information for their geometry. Variable degree of linear polarization was observed in long period recurrent nova RS Oph <Cropper, 1990> as in short period systems: U Sco (Anupama et al. <2013>; Ikeda et al. <2000>) and T Pyx <Pavana et al., 2019>. Variable degree of polarization was detected in nova V339 Del (Shakhovskoy et al. <2017>; Kawakita et al. <2019>) and the classical novae: V705 Cas, V4362 Sgr, V2313 Oph and BY Cir in outburst <Evans et al., 2002>.

In the recurrent nova RS Oph <Cropper, 1990> observed variable linear polarization during 1985 outburst indicating the presence of intrinsic polarization. Observations of RS Oph at quiescence from July 2017 to July 2018 indicate that at this time, there is no intrinsic po-

larization in RS Oph <Nikolov et al., 2019>. Similar to RS Oph at quiescence, as this study demonstrates, in T CrB also is not observed intrinsic polarization. Intrinsic degree of polarization was observed two days after the last outburst of the recurrent nova RS Oph <Nikolov & Luna, 2021>.

Theoretical model describes asymmetry of the ejected material in recurrent nova RS Oph <Booth et al., 2016>. Asymmetry in the ejected material in RS Oph after the nova eruption is well visible in near-infrared (5.5 days after 2006 outburst by Chesneau et al. <2007>), optical (155 and 449 days after 2006 outburst by Bode et al. <2007> and Ribeiro et al. <2009>), radio (21.5 day after 2006 outburst by O'Brien et al. <2006>; 20.8 and 26.8 days after the 2006 outburst by Rupen et al. <2008>), 34 days after the 2006 outburst by Sokoloski et al. <2008>), and X-ray (1254 days after 2006 outburst by Montez et al. <2021>). All observations of asymmetry indicate bipolar structure with East-West orientation. The position angle obtained with spectropolarimetry is aligned with the East-West orientation <Nikolov & Luna, 2021>.

Previous polarimetric observations in V filter of T CrB: $P_V(\%) = 0.37 \pm 0.04$ at $P.A._{obs} = 111^\circ \pm 3^\circ$ <Schulte-Ladbeck, 1985> are similar to reported in this paper. Munari et al. <2016> reported that in 2015 T CrB has entered a super-active phase that is very similar to its state a few years before its nova outburst in 1946, however, Iłkiewicz et al. <2016> argues that this is one of the numerous active phases that T CrB has experienced in the past. It is worth noting that dramatic change in

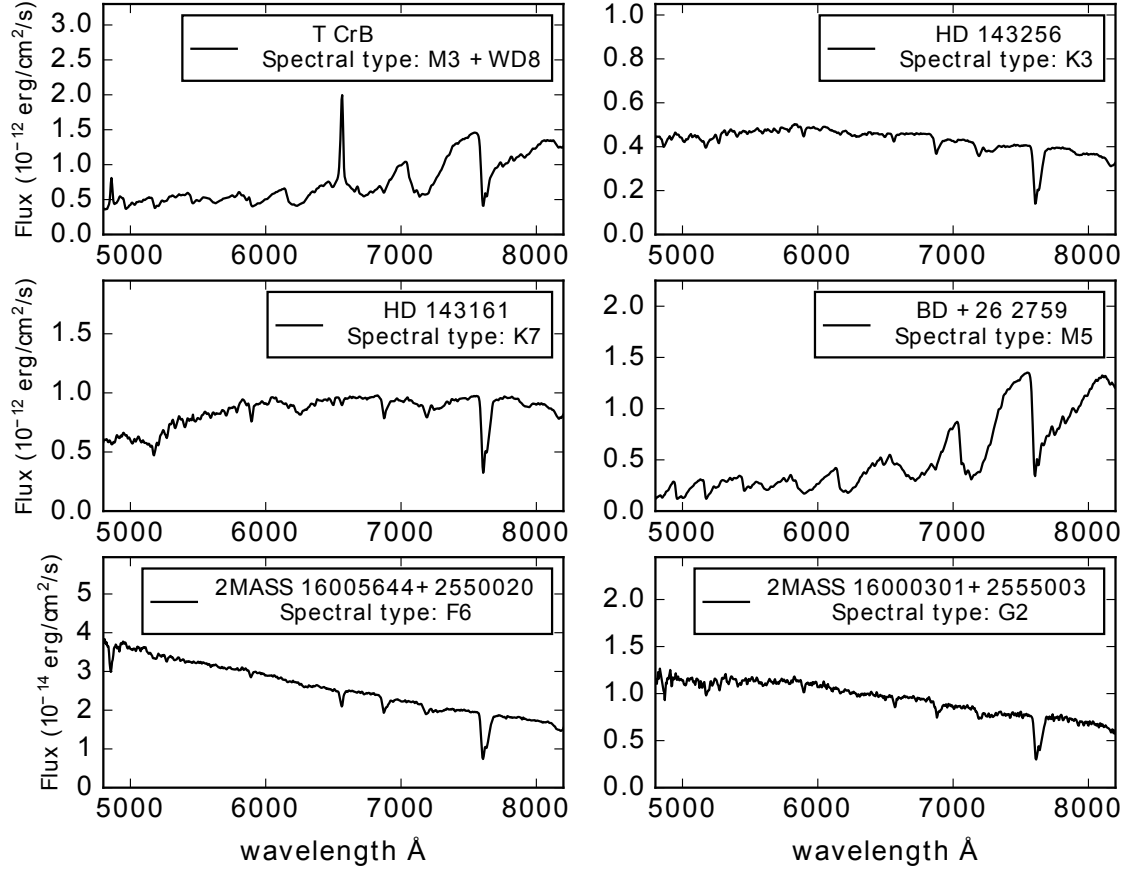


Figure 9: Optical spectra of T CrB and the stars of the direction of T CrB were obtained in 2020-02-02. All fluxes were corrected for interstellar reddening. The absorption features around 7600 Å onwards are due to the atmosphere.

the boundary layer in T CrB was observed by Luna et al. <2018>. Luna et al. <2018> suggest that the 'optical brightening event, which could be a similar event to that observed about 8 years before the most recent thermonuclear outburst in 1946, is due to a disk instability'. Based on an exhaustive historical optical light curve and the pre-eruption-plateau Schaefer <2019> predict that the next eruption of T CrB will be in 2023.6 ± 1.0 , on the other hand, Luna et al. <2020> predict that T CrB is within 3-6 years of its next thermonuclear outburst. Spectropolarimetric observations of RNe at quiescence and after the nova outburst allow determining interstellar and intrinsic component polarization after the nova outburst of the RNe systems. To obtain an intrinsic degree of polarization and position angle of the recurrent nova T CrB shorter after the upcoming outburst <Luna

et al., 2020>, it is necessary to obtain the interstellar polarization toward T CrB. It can be expected that among various observing techniques spectropolarimetry first of all will give information about asymmetry after the nova outburst.

Conclusion

The optical spectropolarimetric observation in range from 4800 Å to 8200 Å of the recurrent nova T CrB are presented in this paper. The results indicated that:

- The maximum of the degree of the linear polarization is $P_{max(obs)}(\%) = 0.46\% \pm 0.01$ at $\lambda \approx 5200$ Å. The position angle is $P.A._{obs} = 100.^{\circ}8 \pm 0.^{\circ}9$. During the period of observations from February

Table 5: Spectral classification

Object	m_v	Distance ^a pc	M_v	Spectral ^b type	BC^c	M_{bol}
T CrB	9.9	887 ⁺¹⁸ ₋₂₉	0.16	M3	-1.97	-2.02
HD 143256	10.1	613 ⁺⁵ ₋₄	0.91	K3	-0.41	0.50
BD +26 2759	10.6	1066 ⁺²⁶ ₋₂₆	0.40	M5	-3.28	-3.05
HD 143161	9.6	759 ⁺⁹ ₋₉	-0.10	K7	-1.00	-1.03
2MASS	12.9	727 ⁺⁸ ₋₇	3.30	F6	-0.05	3.33
16005644+2550020						
2MASS	14.1	919 ⁺¹³ ₋₁₁	3.98	G2	-0.11	3.87
16000301+2555003						

Note:^a - Distance based on Gaia Gaia DR3 <Bailer-Jones et al., 2021>; ^b Spectral type obtained using PyHammer <Kesseli et al., 2017>; ^c - Bolometric correction from Pecaut & Mamajek <2013> Pecaut & Mamajek (2013).

2018 to August 2021 there is no intrinsic polarization in T CrB and the derived values represent the interstellar polarization.

- Based on the degree of polarization the interstellar extinction toward the RNe T CrB is $E_{B-V} \approx 0.07$.
- The degree of polarization in the direction toward T CrB is practically constant at the distance from 400 pc to 1100 pc. This behavior of the degree of polarization between 400 and 1100 pc can be explained with a low-density cavity of the interstellar dust around T CrB. It can be concluded that the polarization toward T CrB is due to the foreground interstellar dust located at the distance up to ≈ 400 pc.
- 3D maps of the polarization and extinction of the stars in the field 10×10 deg. around T CrB are created.
- About the Be star HD 138749 can be expected variable degree of polarization.

The spectropolarimetric observations at quiescence reported here can be useful to investigate intrinsic polarization after the forthcoming outburst.

Acknowledgments

This work is supported by project number KPII-06-MII58/1 -"Spectral and spectropolarimetric characteristics of the interstellar medium", Bulgarian National Science Fund.

I am grateful to Antoaneta Antonova, Radoslav Zamanov, and Gerardo Juan Manuel Luna for their

comments and support. I gratefully acknowledge observing grant support from the Institute of Astronomy and National Astronomical Observatory, Bulgarian Academy of Sciences.

References

- Anupama, G. C. & Mikołajewska, J. 1999, A&A, 344, 177
Anupama, G. C. 2008, RS Ophiuchi (2006) and the Recurrent Nova Phenomenon, 401, 31
Anupama, G. C., Kamath, U. S., Ramaprakash, A. N., et al. 2013, A&A, 559, A121
Bagnulo, S., Landolfi, M., Landstreet, J. D., et al. 2009, PASP, 121, 993.
Bagnulo, S., Cox, N. L. J., Cikota, A., et al. 2017, A&A, 608, A146.
Bailer-Jones, C. A. L., Rybizki, J., Fouesneau, M., et al. 2021, AJ, 161, 147.
Belczynski, K. & Mikołajewska, J. 1998, MNRAS, 296, 77.
Berdyugin, A., Piirola, V., & Teerikorpi, P. 2014, A&A, 561, A24.
Bode, M. F., Harman, D. J., O'Brien, T. J., et al. 2007, ApJ, 665, L63.
Booth, R. A., Mohamed, S., & Podsiadlowski, P. 2016, MNRAS, 457, 822.
Cannon, A. J. & Pickering, E. C. 1993, VizieR Online Data Catalog, III/135A
Cassatella, A., Patriarchi, P., Selvelli, P. L., et al. 1982, Third European IUE Conference, 176, 229
Cardelli, J. A., Clayton, G. C., & Mathis, J. S. 1989, ApJ, 345, 245.
Chesneau, O., Nardetto, N., Millour, F., et al. 2007, A&A, 464, 119.
Clarke, D. 2010, Stellar Polarimetry by David Clarke. Wiley, 2010.
Cox, N. L. J., Boudin, N., Foing, B. H., et al. 2007, A&A, 465, 899.
Cropper, M. 1990, MNRAS, 243, 144.
Evans, A., Yudin, R. V., Naylor, T., et al. 2002, A&A, 384, 504.
Farhang, A., Khosroshahi, H. G., Javadi, A., et al. 2015, ApJS, 216, 33.
Fekel, F. C., Joyce, R. R., Hinkle, K. H., et al. 2000, AJ, 119, 1375.
Fosalba, P., Lazarian, A., Prunet, S., et al. 2002, ApJ, 564, 762.
Jockers, K., Credner, T., Bonev, T., et al. 2000, Kinematika i Fizika Nebesnykh Tel Supplement, 3, 13
Heger, M. L. 1919, PASP, 31, 304
Heiles, C. 2000, AJ, 119, 923.
Hobbs, L. M., York, D. G., Thorburn, J. A., et al. 2009, ApJ, 705, 32.
Ikeda, Y., Kawabata, K. S., & Akitaya, H. 2000, A&A, 355, 256.

- Ikiewicz, K., Mikołajewska, J., Stoyanov, K., et al. 2016, MNRAS, 462, 2695.
- Kawakita, H., Shinnaka, Y., Arai, A., et al. 2019, ApJ, 872, 120.
- Kesseli, A. Y., West, A. A., Veyette, M., et al. 2017, ApJS, 230, 16.
- Luna, G. J. M., Mukai, K., Sokoloski, J. L., et al. 2018, A&A, 619, A61.
- Luna, G. J. M., Sokoloski, J. L., Mukai, K., et al. 2020, ApJ, 902, L14.
- Montez, R., Luna, G. J. M., Mukai, K., et al. 2021, arXiv:2110.04315
- Munari, U., Dallaporta, S., & Cherini, G. 2016, New A, 47, 7.
- Nikolov, Y. M., Zamanov, R. K., & Stoyanov, K. A. 2019, Acta Astron., 69, 361.
- Nikolov, Y. 2020, Bulgarian Astronomical Journal, 32, 125
- Nikolov, Y. & Luna, G. J. M. 2021, The Astronomer's Telegram, 14863
- O'Brien, T. J., Bode, M. F., Porcas, R. W., et al. 2006, Nature, 442, 279.
- Pavana, M., Anche, R. M., Anupama, G. C., et al. 2019, A&A, 622, A126.
- Pecaut, M. J. & Mamajek, E. E. 2013, ApJS, 208, 9.
- Puspitarini, L., Lallement, R., & Chen, H.-C. 2013, A&A, 555, A25.
- Ribeiro, V. A. R. M., Bode, M. F., Darnley, M. J., et al. 2009, ApJ, 703, 1955.
- Rupen, M. P., Mioduszewski, A. J., & Sokoloski, J. L. 2008, ApJ, 688, 559.
- Schaefer, B. E. 2009, ApJ, 697, 721.
- Schaefer, B. E. 2010, ApJS, 187, 275.
- Schaefer, B. E. 2019, American Astronomical Society Meeting Abstracts #234
- Schlegel, D. J., Finkbeiner, D. P., & Davis, M. 1998, ApJ, 500, 525.
- Schmidt, G. D., Elston, R., & Lupie, O. L. 1992, AJ, 104, 1563.
- Schulte-Ladbeck, R. 1985, A&A, 142, 333
- Serkowski, K., Mathewson, D. S., & Ford, V. L. 1975, ApJ, 196, 261.
- Shakhovskoy, D. N., Antonyuk, K. A., & Belan, S. P. 2017, Astrophysics, 60, 19.
- Sokoloski, J. L., Rupen, M. P., & Mioduszewski, A. J. 2008, ApJ, 685, L137.
- Stanishev, V., Zamanov, R., Tomov, N., et al. 2004, A&A, 415, 609.
- Tody, D. 1993, Astronomical Data Analysis Software and Systems II, 52, 173
- Turnshek, D. A., Bohlin, R. C., Williamson, R. L., et al. 1990, AJ, 99, 1243.
- Whittet, D. C. B. & van Breda, I. G. 1978, A&A, 66, 57
- Whittet, D. C. B. 2003, Dust in the galactic environment